An Automated Embedded Computer Vision System for Object Measurement

Nicholas Pauly
Electrical and Computer Engineering
Boise State University
Boise, Idaho 83706
research@nickpauly.com

Nader I. Rafla, Ph.D., P.E.,
Department of Electrical and Computer Engineering
Boise State University
Boise, Idaho 83706
nrafla@boisestate.edu

***Abstract*— Automation is common in many industries. Some tasks, such as object measurement, can easily be automated. The equipment required to perform automated measurements may be cost prohibitive and may prevent widespread deployment in automated point of sale kiosks or product inspection applications. This paper focuses on the development of an optical measurement device that is inexpensive relative to existing systems. The device consists of an image sensor, several laser line projectors, and a microcontroller. The hardware design and configuration of the device is discussed along with the algorithms used to process the captured images and perform the measurement tasks. The conclusion includes a discussion of the performance of the optical measurement device.**

Keywords—Automation; Hough Transform; Image Processing; Object Measurement

I. INTRODUCTION

Many measurements can be performed by using a tape measure, ruler, caliper, or other measurement tools. One of the drawbacks to using these methods is that they require contact with the item being measured. The contact may damage the object surface or cause the object to deform. For example, as soon as a silicone keypad is touched by a measurement device, such as calipers, the silicone deforms, making the measurement less accurate than if an optical measurement device (OMD) is used.

In addition to overcoming some of the previously described issues arising from the use of contact measurement devices, the measurement speed can be improved and data recording can be automated. The OMD presented in this paper does not require precise placement of the object being measured within the OMD field of view. Due to the flexibility of the object placement, overall measurement speed can increase. Since the proposed OMD is automated and computer controlled, it can easily save measurement data in a database. Automatic data collection is quicker and less prone to error than having an operator manually enter the data into a software program.

The OMD presented in this paper was designed and built specifically for performing measurement operations. Hardware was designed and built to support the operation of an image processing algorithm based on the Hough Transform. The algorithm is used to detect laser lines in an image and calculate the size of an object based on the locations of the laser lines. Firmware was written to control all of the hardware components and to implement the image processing algorithm. In addition to the firmware, software was developed to interface a PC to the OMD for the purpose of debugging and device control. This paper focuses on the design and implementation of the OMD.

II. DISTANCE MEASUREMENT

Several distance measurement methods were evaluated for use in the OMD. Prior to settling on an image based range finding method, several ultrasonic rangefinders and an infrared rangefinder were evaluated. Due to consistency and accuracy errors encountered with the dedicated rangefinders, an image based approach was explored. Multiple image based distance measurement methods are described in literature that use various methods to determine the distance to an object [1-9]. The measurement method developed for the system described in this paper is based on the laser dot projection methods described in [8] and [9].

An angled laser aiming configuration similar to the one described in [9] was selected for use in the OMD because it provided better measurement resolution than the one described in [8]. In addition to the narrow camera field of view, the angled laser aiming method also has the benefit of the projected lasers lines physically moving away from each other as the height of the measured object increases. The OMD lasers are positioned 114mm from the center of the camera lens. The laser position was carefully chosen to allow the camera and lasers to be mounted in a 200mm x 200mm enclosure.

III. HARDWARE

The OMD hardware consists of an enclosure containing four laser line projectors, laser control circuitry, a 5MP monochrome image sensor, a lens, and a 400MHz ARM microcontroller. The OMD hardware is shown in Fig. 1. Several lenses with focal lengths of 4mm, 6mm, 8mm, and 12mm were evaluated to determine the optimal focal length. A short focal length allows for a large field of view with limited measurement resolution. A longer focal length allows for greater measurement resolution at the cost of limiting the field of view and the size of the object that can be measured.

978-1-4799-0066-4/13/$31.00

Fig. 1. Optical Measurement Device Hardware

A lens focal length of 6mm was selected as the optimal focal length to use. Selection of the optimal focal length required several tradeoffs. To allow for larger objects to be measured, some measurement resolution must be traded off in favor of a larger field of view. To allow for sufficient measurement resolution, the field of view must be reduced. A lens focal length of 6mm allows for sufficient measurement resolution with a relatively large field of view.

IV. Image Processing Algorithm

A. Overview

The image processing algorithm begins by capturing two images of the object being measured. The first image that is captured *does not* have the laser line projectors turned on. The second image that is captured *does* have the laser line projectors turned on. After these two images are captured, they are compared with each other to find the pixels where laser lines are present. The resulting image from the comparison is a bi-level image consisting primarily of the laser lines as shown in Fig. 2. In addition to the laser lines, there is a significant amount of image noise. After filtering the noise, a line detection algorithm is run to detect the laser lines in the image. The size of the object being measured is calculated using data derived from the laser lines in the image.

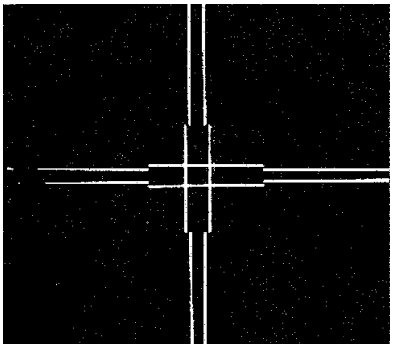

Fig. 2. Bi-level Comparison Image

B. Line Detection

The line detection and processing algorithm needs to be robust and immune to small image imperfections, such as broken lines and noise. Ideally, it should be able to process laser lines that are not perfectly aligned with the horizontal and vertical image axes. The algorithm also needs to be optimized to run on a microcontroller with limited processing power and memory. The line detection and processing algorithm that was designed and implemented in the OMD meets these criteria.

The first step of the algorithm is performed using the Hough Transform (HT) feature extraction technique. The HT was originally proposed by Paul Hough [10]. Its practical applications are described in [11] and [12]. Optimizations have been made to increase the algorithm processing speed while reducing memory usage. For example, the HT implementation used for the OMD is tuned to only detect horizontal and vertical lines since other line angles do not need to be recognized for the OMD to operate.

C. Line Filtering

After the line detection step has been completed, the data in the Hough Transform Accumulator (HTA) can be processed to determine the locations of the laser lines in the image. The first HTA data processing step checks all of the HTA bin count values and discards all of the bins that do not exceed a preset bin count threshold value. After the threshold is applied, a large number of accumulator bins that contain invalid line data remain. The bins containing invalid line data need to be discarded using methods other than the application of the bin count threshold as discussed below.

The line filtering algorithm makes some assumptions concerning the data in the HTA bins. If lines that are represented by multiple HTA bins are similar, it is assumed that only the bin with the highest count value is valid, similar lines with lower count values are discarded.

The line filtering algorithm uses two lists of lines; the filter list and the valid line list. The filter list contains the HTA bin data sorted in descending order according to the count value. The valid line list contains data for lines that have been determined to be valid.

The line filtering algorithm starts with the bin in the filter list containing the highest count value, called the *reference bin*. Three line parameters from the reference bin are used to test for similar lines; magnitude, angle, and slope. Each parameter has an experimentally determined value which is added or subtracted to/from it to generate a *similarity threshold range*. After the similarity threshold ranges have been calculated, the reference bin is removed from the filter list and added to the valid line list. Next, the line parameters from the bin in the filter list with the highest count value are compared with the reference bin parameters. If none of the parameters fall within the similarity threshold range of the reference bin, no action is taken and the bin with the next highest count value in the filter list is checked. If at least one of the line's parameters falls within the similarity threshold range of the reference bin, an analysis is performed to determine if that line intersects the reference line within a specified field of view. If a line intersection is detected, the bin is discarded from the filter list. The comparison process continues until all of the bins in the filter list have been compared with the reference bin. The filter process is repeated until all of the bins have been removed from the filter list. After the lines represented by the HTA bins have been filtered, they are grouped into horizontal and vertical line groups.

D. Line Data Processing

After the line data is filtered and grouped, the resulting lines are processed to find the line endpoints on the *x-y* plane. Starting from the center of the image, a search is made for the endpoints of the line that is being processed. The line endpoint search is made in both directions along the axis. For each point along the *x* axis that is analyzed, the associated *y* value is calculated to determine the *x-y* coordinate of the pixel that should be read. Similarly, for each point along the *y* axis that is analyzed, the associated *x* value is calculated to determine the *x-y* coordinate of the pixel that should be read. If the pixel at the calculated coordinate is active, the next *x-y* coordinate is calculated and the process continues until an inactive pixel is found. When an inactive pixel is found along the line, one of three cases is possible: case 1 is a break in the line; case 2 is the end of the line; and case 3 is a calculated line divergence from the actual laser line as illustrated in Fig. 3.

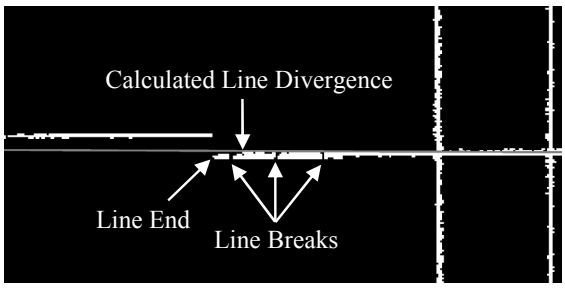

Fig. 3. Inactive Pixel Cases

When an inactive pixel is found, the pixels above and below the inactive pixel are checked to see if they are active. The number of pixels checked are in what is called the *search width* of the line which is determined experimentally. If an active pixel is found above or below an inactive pixel, the search continues as if the *x-y* coordinate containing an inactive pixel had contained an active pixel. A search must be made above and below the calculated *x-y* coordinate because the calculated line parameters may not always exactly match the laser line in the image. The wide search width is especially useful toward the end of the laser line as the calculated *x-y* line coordinates may begin to drift away from the actual laser line.

If the line endpoint search algorithm does not find any active pixels within the search width area, the last *x-y* coordinate is stored as a potential line end coordinate and the line endpoint search continues along the axis a pre-determined number of pixels called the *search distance*. If any active pixels are found within the search distance, the line endpoint search continues as if active pixels had been found continuously along the line. The search distance parameter accommodates line breaks with gaps smaller than the search distance. As with the search width, the search distance is found experimentally. If no active pixels are found within the search width area or the search distance area, it is assumed that the line endpoint has been found. The stored *x-y* coordinate of the last active pixel on the line is saved as the line endpoint. The line endpoint search is performed in both directions starting from the center of the image.

E. Object Size Calculation

The physical size of the object within the OMD field of view is calculated using the data generated by the line detection and processing algorithm. The height of the object must be calculated before the length and width of the object because the length and width calculations depend on the height value. The calibration data used to determine the height, the length, and the width of the object is found experimentally. Calibration data is gathered by capturing images of an object with a known length and width at multiple known heights.

For each height, the pixel distance between the parallel laser lines is recorded along with the pixel lengths of the lines projected onto calibration object. The data gathered from the calibration process is used to derive two equations. The first equation is used to calculate the height of an object, in millimeters, based on the number of pixels between the parallel laser lines. The second equation is used to determine the length and the width of the object, in millimeters, given the object height along with the object length and width in pixels.

The lengths of the two horizontal lines projected on the object are averaged to determine the object width in pixels. Likewise, the lengths of the two vertical lines are averaged to determine the length of the object in pixels. The laser lines projected onto the object being measured break when there is an abrupt change in object height. Typically, laser line breaks occur on the edge of the object where there is a height change from the object surface to the background surface. The boundaries of the laser line breaks represent the edges of the object. The endpoints of the laser lines projected on the object being measured are used to determine the object perimeter. The currently implemented object measurement method only works for rectangular objects.

V. Experimental Results

A. Speed

Image capture and processing speeds depend on several variables including the image exposure time and capture resolution. The exposure time for the image capture is dictated by the ambient lighting around the OMD and the lens aperture. A longer exposure time will increase the total image capture time. Higher image capture resolutions also increase the image capture time and require more data to be transferred to, and processed by, the microcontroller than lower resolution image captures.

Table I shows the average image capture and processing times for the three image capture resolutions supported by the OMD. The total capture and processing time for a 480x480 pixel image averages 791.2ms. This speed subjectively feels fast and gives the user almost instant feedback. Unfortunately, as the image capture resolution increases, the total capture and processing time increases. The capture and processing of a 960x960 pixel image takes approximately two seconds to complete which feels relatively slow to the end user. Finally, the 7sec. capture and processing time of a 1920x1920 pixel image would not be desirable to the end user.

TABLE I. AVERAGE IMAGE CAPTURE AND PROCESSING TIMES

Processing Step	Image Resolution		
	480x480	***960x960***	***1920x1920***
Image Capture	93.7 ms	92.5 ms	171.7 ms
Image Comparison	60.8 ms	222.3 ms	870.2 ms
Noise Filter	156.0 ms	615.4 ms	2450.6 ms
Hough Transform	271.4 ms	862.0 ms	3294.2 ms
Data Processing	115.6 ms	123.5 ms	160.0 ms
Total	791.2 ms	2008.3 ms	7118.5 ms

The image subtraction, noise filter, and Hough Transform image processing steps process each pixel in the captured image. The amount of time required to perform these steps increases by approximately four times when the image resolution is doubled due to the four times increase in captured image data.

Reducing the image capture resolution increases the image capture and processing speed. The reduced amount of data associated with a lower resolution image capture reduces the potential accuracy of the OMD. The next section discusses the OMD resolution and accuracy for the three supported image capture resolutions.

B. Measurement Resolution and Accuracy

The measurement resolution and accuracy of the OMD varies depending on several factors including the focal length of the lens, the capture resolution, and the object distance from the lens. In addition to the measurement resolution defined by the focal length and image capture resolution, the consistency between captured images can affect the measurement accuracy. Image noise can cause the laser lines found by the line detection and processing algorithm to vary by several pixels between image captures. The reflectivity of different objects of the same size can also affect the consistency and accuracy of the object measurements.

Table II shows the errors associated with the measurements taken with the calibrated OMD. All of the measurements were performed using a 6mm focal length lens. The table shows the actual object measurement next to the measurement returned by the OMD along with the measurement error.

TABLE II. MEASUREMENT ERROR FOR 960X960 IMAGE IN MM

Measured Height	Actual Height	Height Error	Measured Length	Actual Length	Length Error
-1.52	0.00	1.52	---	---	---
1.78	3.05	1.27	---	---	---
20.32	27.94	7.62	---	---	---
51.05	53.09	2.03	307.09	304.80	-2.29
77.72	77.98	0.25	305.56	304.80	-0.76
101.35	103.12	1.78	304.29	304.80	0.51
128.78	128.02	-0.76	303.53	304.80	1.27
152.40	152.91	0.51	305.05	304.80	-0.25
177.29	178.05	0.76	306.07	304.80	-1.27
200.91	202.95	2.03	306.83	304.80	-2.03

VI. CONCLUSION

The OMD is capable of consistently measuring an object with an accuracy of at least ±3.0mm using a 1920x1920 pixel image capture resolution and a 6mm focal length lens. This highest measurement accuracy of the OMD comes at the cost of increased image capture and processing time. To achieve a reasonable balance between accuracy, image capture time, and image processing time, the 960x960 pixel image capture resolution is recommended. Experiments have shown that the measurement error is typically less than ±2.03mm when a 960x960 pixel image capture is used.

The OMD is entirely self-contained. The image capture, image processing, and measurement calculation operations are all performed within the OMD. A host PC is only required for triggering measurement operations and displaying the results. The device can quickly perform measurements when the image capture resolution is set to 480x480 pixels. In this case, the device can perform up to 1.25 measurement operations per second. The recommended image capture resolution of 960x960 pixels results in a measurement speed of approximately 0.5 measurement operations per second.

REFERENCES

[1] M. Lu, C. Hsu, Y. Lu, "Distance and Angle Measurement of Distant Objects on an Oblique Plane Based on Pixel Variation of CCD Image," in *Instrumentation and Measurement Technology Conf.*, Austin, TX, 2010, pp. 318-322.

[2] C. Hsu, M. Lu, K. Chin, "Distance Measurement Based on Pixel Variation of CCD Images," in *Proc. of the 4th Int. Conf. on Autonomous Robots and Agents*, Wellington, New Zealand, 2009, pp. 324-329.

[3] T. Wang, M. Lu, C. Hsu, Y. Lu, C. Tsai, "Three dimensional distance measurement based on single digital camera," in *Proc. 2007 WSEAS Int. Conf. on Circuits, Syst., Signal and Telecommun.*, Gold Coast, Australia, 2007, pp. 153-157.

[4] H. Kim, C. Lin, J. Song, H. Chae, "Distance Measurement Using a Single Camera with a Rotating Mirror," *Int. J. of Control, Automation, and Syst.*, vol. 3, no. 4, pp. 542-551, Dec. 2005.

[5] Z. Liu, T. Chen, "Distance Measurement System Based on Binocular Stereo Vision," in *Int. Joint Conf. on Artificial Intelligence*, Hainan Island, China, 2009, pp. 456-459.

[6] L. Xiaoming, Q. Tian, C. Wanchun, Y. Xingliang, "Real-Time Distance Measurement Using a Modified Camera," in *Sensors Applications Symp.*, China, 2010, pp. 54-58.

[7] T. Tsukiyama, "Measuring the distance and orientation of a planar surface using nonstructured lighting-3-D measurement system for indoor mobile robots," *IEEE Trans. Instrum. Meas.*, vol. 45, no. 5, pp. 885-893, Oct. 1996.

[8] C. Chen, M. Lu, C. Chuang, C. Tsai, "Vision-Based Distance and Area Measurement System," *Int. J. of Circuits, Syst. and Signal Process.*, vol. 1, no. 1, pp. 28-33, 2007.

[9] M. Lu, W. Wang, H. Lan, "Image-based height measuring systems for liquid or particles in tanks," in *2004 IEEE Int. Conf. on Networking, Sensing and Control*, Taipei, Taiwan, 2004, pp. 24-29.

[10] P. Hough, "Method and Means for Recognizing Complex Patterns," U.S. Patent 3 069 654, Dec. 18, 1962.

[11] R. Gonzalez and R. Woods, *Digital Image Processing*, 2nd ed. Upper Saddle River, NJ: Prentice Hall, 2002.

[12] R. Duda and P. Hart, "Use of the Hough Transformation To Detect Lines and Curves in Pictures," *Graphics and Image Processing*, vol. 15, no. 1, pp. 11-15, Jan. 1972.